Essential Readings in Light Metals: Aluminum Reduction Technology.
Edited by Geoff Bearne, Marc Dupuis and Gary Tarcy.

SULFUR AND FLUORINE CONTAINING ANODE GASES PRODUCED DURING NORMAL ELECTROLYSIS AND APPROACHING AN ANODE EFFECT

Mark M.R. Dorreen, Darrell L. Chin, Jackie K.C. Lee, Margaret M. Hyland and Barry J. Welch

Department of Chemical and Materials Engineering
The University of Auckland
Private Bag 92019, Auckland, New Zealand

Abstract.

The gases evolved from a laboratory scale alumina reduction cell were monitored with a mass spectrometer to determine the species present and qualitatively how they varied. In conjunction with the gas analysis, thermodynamic predictions were made of the range and composition of the gases produced under different conditions.

Carbonyl sulfide was evolved at a steady rate during normal electrolysis, but no SO_2 was detected. Thermodynamic predictions indicate that when the crust is broken or the cell gas is burned SO_2 is dominant.

The production of CF_4 and C_2F_6 did not start until anode effect, and while small amounts of C_2F_6 could not be differentiated from CF_4 in the technique used, it was evident that CF_4 dominated. Carbonyl fluoride was detected in the period shortly before anode effect, this period ranging up to 5 minutes. Thermodynamic analysis supports the formation and subsequent decomposition of COF_2, suggesting this leads to the initiation of an anode effect.

Introduction and Literature.

There has been a strong focus on the gaseous electrochemical products of aluminium smelting since the 1990 Rio Conference on the environment. The aluminium smelting process emits significant volumes of carbon oxides, sulfur containing species, and during anode effect, perfluorocarbons also. More research effort is now being put into investigating formation conditions in order to develop minimisation strategies.

While the environmental impact of aluminium smelting emissions has only been recognised recently, data on the gas composition has been available since at least the 1950's. Henry and Holliday [1] sampled gases from both Söderberg and prebaked anode cells, and looked at slightly burned and nearly completely burned gas during normal electrolysis and anode effect. They showed that the gas composition was basically the same for the different cell types. CF_4 and C_2F_6 were only detected during anode effect, with C_2F_6 being minimal. During normal electrolysis COS was detected in the unburnt gas, whereas SO_2 was dominant in burnt gas. H_2S was only seen in very small amounts, and CS_2 was detected in unburnt anode effect gas only.

The anode effect phenomenon has been reported on in many studies [3,5,7,8]. The production of CF_4 and C_2F_6 and the global warming potential of these gases was discussed. The common findings were that C_2F_6 is evolved at a much lower rate than CF_4, and that C_2F_6 is only evolved immediately at the start of the anode effect and does not continue for as long a period as CF_4. These perfluorocarbons were not detected during normal electrolysis except when the bath ratio was extremely low [9], when they were detected at normal cell voltages, apparently due to the higher fluoride activity of the electrolyte.

Similar results were reported by Øygård et al. [4] for studies of laboratory and industrial cells. They discuss the possibility of COF_2 formation, although none was detected. They also show traces of CF_4 detected immediately before an anode effect, possibly formed directly or by decomposition of COF_2. Berge et al. [6] also discussed formation and decomposition of COF_2, but gave no direct evidence.

There is little doubt of the negative aspects of anode effects, demonstrated simply by the amount of research into understanding them better, and also by the Voluntary Aluminum Industrial Partnership formed between the U.S. Environmental Protection Agency and primary aluminium producing companies aiming to reduce annual PFC emissions from smelters by 45% of 1990 levels by 2000. However there are positive aspects of the anode effect phenomenon as well, such as burning off anode carbon projections, removing carbon dust, increasing the dissolution of sludge, "cleaning up" the cell and initialising cell feeding and control strategies [10].

Oedegard et al. [2] analysed the COS, CS_2 and SO_2 emissions from a laboratory cell and made thermodynamic calculations based on a series of reactions involving sulfurous species. The laboratory cell showed the gas production in the order of COS > SO_2 > CS_2. The calculations showed SO_2 preferred at 1250K and higher CO_2/CO ratios, otherwise COS was the major sulfur containing gas. Similar results were found in industrial prebaked anode cells, showing about 96% of the sulfur emitted as SO_2 and only about 4% as COS [13]. Gas sampled directly from the anode had similar amounts of COS and CS_2, but gas sampled from the exhaust duct has a COS/CS_2 ratio of 50:1, indicating the CS_2 being oxidised by air as it moves from anode to duct.

In 1995 Harnisch et al. [11] put forward evidence to suggest that aluminium smelting is a significant source of atmospheric carbonyl sulfide. This gas has a long atmospheric life and reacts with water to form sulfuric acid which catalyses reactions of ozone destruction. In a subsequent publication [12], an estimate was made of the global average emissions of environmentally harmful gases from aluminium smelting. It was also estimated that in 1995 aluminium production was responsible for about 6% of all COS emissions and about 20% of the anthropogenic share.

The scope of the work presented here ranges from thermodynamic predictions of the gaseous species formed in the aluminium smelting cell, to a laboratory scale electrolytic investigation to detect species formed under controlled conditions. The laboratory study is only performed to an approximate level of quantitative analysis.

Thermodynamic Predictions.

Listed below are electrochemically based reactions that have been predicted at 970°C. Although (1) is thermodynamically preferred, in practice the reaction kinetics and polarisation result in the gas formed under the anode exceeding 90% CO_2 (2). The CO formation becomes more important in the lower current density regions on the sides of anodes. It is well known that as the alumina concentration decreases the anode potential increases through polarisation until an anode effect is reached. The thermodynamic analysis shows that the formation of COF_2 may occur (reaction 3) at a potential significantly below that for the electrochemical evolution of CF_4 and C_2F_6 (reactions 4 and 5), however.

$$3C + Al_2O_3 = 2Al + 3CO \qquad E° = -1.06V \ (1)$$

$$3C + 2Al_2O_3 = 4Al + 3CO_2 \qquad E° = -1.18V \ (2)$$

$$2Na_3AlF_6 + Al_2O_3 + 3C = 3COF_2 + 6NaF + 4Al \qquad E° = -1.86V \ (3)$$

$$4Na_3AlF_6 + 3C = 12NaF + 4Al + 3CF_4 \qquad E° = -2.54V \ (4)$$

$$2Na_3AlF_6 + 2C = 6NaF + 2Al + C_2F_6 \qquad E° = -2.78V \ (5)$$

In the presence of sulfur the formation of COS theoretically would occur at a potential below that for the formation of either or CO or CO_2 according to reaction 6. If COS does not form by an electrochemical mechanism, then as seen by reactions 7 and 8 it can be formed chemically because of the strongly favoured chemical equilibria. If COF_2 was formed by the electrochemical reaction given above, it would be thermodynamically unstable in the presence of carbon as illustrated by the equilibria given for reaction 9. Likewise, some C_2F_6 may also be formed by a similar reaction (10). Because of this one would not expect to detect high concentrations of COF_2.

$$Al_2O_3 + 3C + 3S = 3COS + 2Al \qquad E° = -1.04V \quad (6)$$

$$S + CO_2 + C = COS + CO \qquad K = 4.44E+02 \quad (7)$$

$$CO + S = COS \qquad K = 4.57E+00 \quad (8)$$

$$2COF_2 + C = 2CO + CF_4 \qquad K = 8.64E+01 \quad (9)$$

$$3COF_2 + 2C = 3CO + C_2F_6 \qquad K = 1.17E-03 \quad (10)$$

Boron nitride shielding was used in the laboratory cell to clearly define the current path. As discussed in the results below, some boron containing gasses were found at the anode effect and it is interesting to note that the most thermodynamically favoured reactions for this are 11 and 12.

$$3COF_2 + 2BN = 2BF_3 + 3CO + N_2 \qquad K = 9.22E+32 \quad (11)$$

$$6CF_4 + 2BN = 2BF_3 + C_2F_6 + N_2 \qquad K = 3.80E+12 \quad (12)$$

Of significance in the overall thermodynamic analysis is the formation of carbonyl fluoride (reaction 3) and its decomposition (reaction 9). Calandra et al. [16] detected this in sweep voltammetry but there have been no reportings of carbonyl fluoride being chemically detected. Because of the depolarising effect of reaction 9, one could predict that an anode effect could occur at a total anode polarisation of less than 0.7 volts. Generally, the industry assumes the combination of anode bubble resistance and polarisation accounts for 0.5 of a volt. However, if proper account is taken of the bubble resistance [17] the normal anode polarisation would be 0.4 volts. Consequently, an increase in anode potential of approximately 0.4 volts or less would cause the onset of an anode effect by the reaction combination.

Figure 1 presents a voltage-time track of an operating smelter cell as it approaches an anode effect. From this it is seen that the increase in voltage from the minimum is less than 0.4 of a volt up to 5 seconds prior to the onset of an anode effect. Several similar curves have been analysed, showing the increases range from 0.2 to 0.4 of a volt. This observation, if the

formation of carbonyl fluoride can be confirmed, would provide an explanation of the suddenness of an anode effect at low anode potentials.

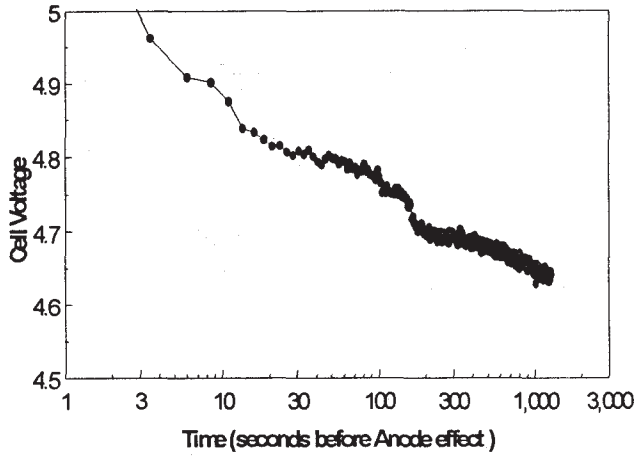

Figure 1: Industrial cell voltage increase before anode effect.

Equipment & Procedure.

The equipment used for the practical experiments was developed for a previous study [14], where a detailed description can be found. Briefly, a laboratory furnace was used to house a small scale cell, electrolysis was performed, the gases produced were continuously flushed from the cell and analysed with a mass spectrometer.

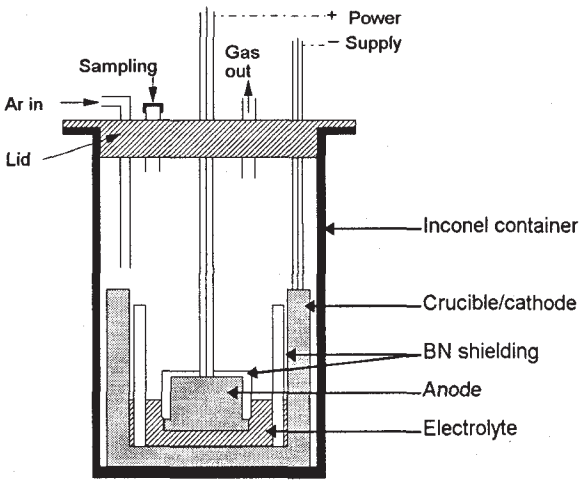

Figure 2: Electrolysis cell, furnace container and lid.

The cell is shown in Figure 2, illustrating BN shielding on the sides of the cathode to eliminate horizontal current and increase the cathodic current density, and over the top of the anode to reduce reactions with exposed carbon. The carbon anode is suspended into the electrolyte from the lid above, which also has gas inlet and outlet ports for continuous argon purging of the cell. The lid provides a gas tight seal with the inconel container, which is placed inside the furnace. The gas from the cell was scrubbed by passing it through a fluidised bed of primary alumina to remove particulates before being introduced to the mass spectrometer.

Thermodynamic analysis was made using the CSIRO Thermochemistry program operated in CHEMIX mode, using the standard free energy minimisation approach.

Experimental Conditions.

The laboratory cell was operated with a typical electrolyte composition of 9wt% excess AlF_3, 4wt% CaF_2 with starting Al_2O_3 concentrations from 6-8wt%. Anode-cathode spacing was 30mm, and anode current density was 1.107A/cm^2 (total current 75A). Cell temperature was 965-985°C. Electrolysis was performed until the cell reached anode effect. It was left to run on anode effect for a short period before the electrolysis power supply was switched off.

The thermodynamic predictions were made by placing material balance limits on the appropriate feedstocks, and considered the scenarios of the laboratory cell and an industrial cell, operating with normal electrolysis and on anode effect. For the industrial cell scenario unburnt, partially burnt and fully burnt anode gases were considered. This then covered the zones in the cell of gas formed under the anode, gas trapped under the crust in a reducing region, and gas emerging through holes and cracks in the crust as burning flames reacting with oxygen in the potroom air. For normal electrolysis the C-O-S system was used, and for anode effect C-O-S-F was used. In both cases the appropriate sulfur to carbon ratio as exists in anodes was used.

Results and Discussion.

Laboratory Cell.

Figure 3 shows the gas analysis data for an experiment, illustrating the change from normal electrolysis to anode effect. Electrolysis was started at 0 minutes, and anode effect was reached after 105 minutes.

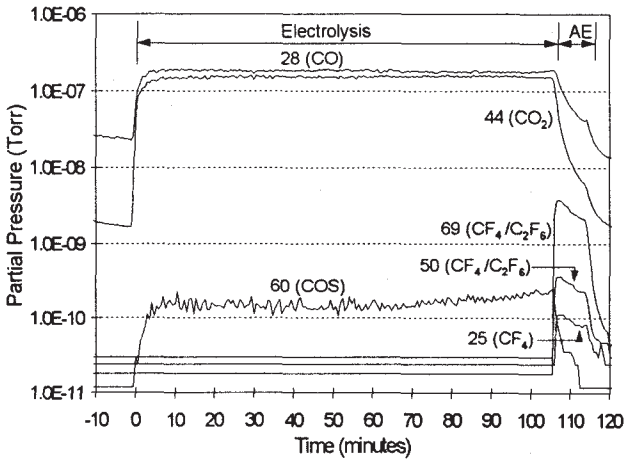

Figure 3: Gases during electrolysis and anode effect.

The upper curves are of carbon monoxide (mass/charge 28) and carbon dioxide (m/e 44). These both dropped away during anode

effect as equipment limitations meant that during an AE the cell current could not be maintained. However during the anode effect the ratio of CO to CO_2 increased dramatically, a trend clearly shown by Tabereaux [5]. The only sulfurous species detected from the laboratory cell was carbonyl sulfide, at m/e 60, shown clearly being formed during electrolysis but falling away during anode effect.

Other sulfurous species targeted were SO_2 at m/e 64 and CS_2 at m/e 76. No response to these was detected at any time, during either normal electrolysis or anode effect. Neither was any S_2 detected. Although predicted, it would condense in the gas collection system and therefore not reach the detector of the mass spectrometer.

Three curves are shown rising at anode effect. These are the CF_3^+ ion at m/e 69, CF_2^+ ion at m/e 50 and CF_2^{2+} ion at m/e 25. Both CF_4 and C_2F_6 give ions at m/e 69 and 50 and it is not possible to differentiate between them. However C_2F_6 does not produce a fragment at m/e 25, so that ion is only from CF_4. The relative intensities of the three ions agree well with the established fragmentation pattern for CF_4 [15]. Thus while C_2F_6 cannot be discounted, if any is present it is only in small amounts, agreeing with other studies. Obviously, no conclusions can be made about the relative rates of formation of CF_4 and C_2F_6.

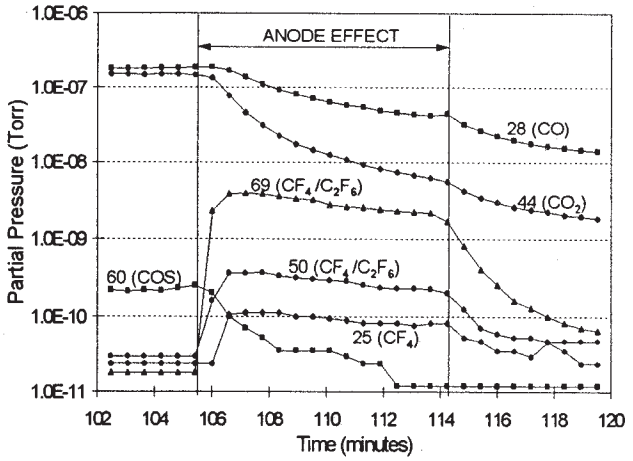

Figure 4: Gases at onset of anode effect.

Figure 4 shows the gases at the onset of anode effect in more detail. The start of the anode effect was defined as the point at which the cell voltage instantaneously rose from the normal operating level to 20V, the power supply limit. It is quite clear that no CF_4/C_2F_6 was produced before this point. The residual gas analyser had a very rapid response time (in these experiments <5 seconds), and in 20 repeat experiments CF_4/C_2F_6 were never detected prior to anode effect. CF_4 was quantified and could be detected to levels at least as low as 0.05mol%.

Other masses were targeted to determine the other species formed in the cell. Figure 5 shows the trace for ions corresponding to COF_2. The curve at m/e 69 of CF_4 and C_2F_6 is shown to define the anode effect starting point, at 60 minutes. The other two curves indicate that COF_2 was formed, and this formation started in the last few minutes before anode effect. The trace at m/e 47 corresponds to COF^+, and 66 corresponds to COF_2^+. The intensity ratio of m/e 47/66 also agrees with the fragmentation pattern of COF_2. In almost all experiments the amount of CO increased as anode effect approached, which could be due in part to the decomposition of COF_2 according to reactions 9,10 and 11, although CF_4 and C_2F_6 were not detected before anode effect.

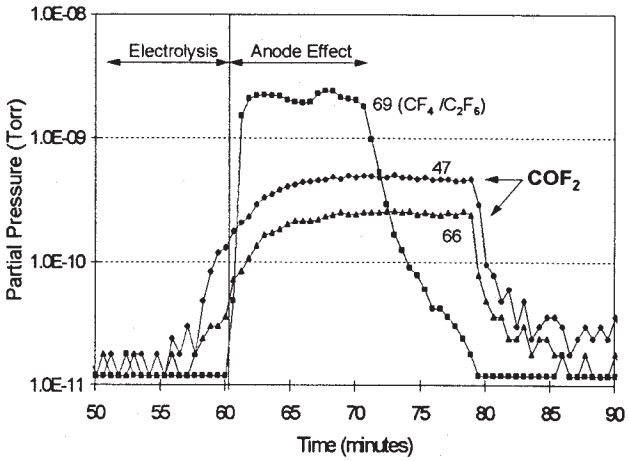

Figure 5: Formation of COF_2.

COF_2 was detected before anode effect in five experiments. Two at 0.295A/cm^2 showed COF_2 produced for a longer period prior to anode effect than the other three at the higher current density of 1.107A/cm^2.

Gas Composition Predictions.

Table 1 gives the predicted composition of the gas under normal electrolysis conditions at 975°C. For the laboratory cell scenario the levels of CO and CO_2 are almost the same, with COS being the dominant sulfurous species. Approximately the same distribution is seen for unburnt industrial cell gas, although there is also some H_2S present as the industrial cell scenario includes H_2 and H_2O from moisture in the air. The partially burnt industrial cell gas only really differs in that the CO_2 has increased and the CO has decreased, although the amounts of S_2 and SO_2 have increased marginally. The totally burnt gas shows a significant change, with CO almost non-existent, CO_2 being the main gas, with SO_2 being the major sulfurous species. This indicates that most of the sulfur in the anodes is initially evolved as COS, increasing the net carbon consumption, and that SO_2 is primarily formed by a secondary burning reaction as the gases emerge from the cell and react with oxygen. A very small trace of CS_2 is seen in all cases, which gets much smaller as the gas is more burnt.

Table 2 gives the predicted gas composition at 975°C for anode effect conditions. For the laboratory cell scenario CO and CF_4 are dominant, with small amounts of COS, CS_2 and COF_2. Only minimal trace of S_2, SO_2 and C_2F_6 are seen. Almost exactly the same composition is seen for unburnt and partially burnt industrial cell gas. Again, CO and CF_4 are dominant. The composition changes as the gas becomes totally burnt. CO_2 is present at nearly the same level as CO, CF_4 has decreased and more COF_2 is present.

Table 1: Predicted gas composition (mol fraction) for normal electrolysis.

	Laboratory Cell	Industrial Cell Unburnt	Industrial Cell Partially burnt	Industrial Cell Totally burnt
CO_2	0.497	0.466	0.599	0.889
CO	0.479	0.484	0.351	2.0E-07
COS	0.018	0.013	0.012	2.3E-19
S_2	0.005	0.003	0.004	5.0E-24
CS_2	1.5E-04	8.7E-05	5.3E-05	1.4E-38
SO_2	4.3E-05	2.7E-05	1.0E-04	0.025
O_2	2.8E-15	2.4E-15	7.6E-15	0.054
H_2	0	0.010	0.007	4.5E-09
H_2O	0	0.015	0.019	0.032
H_2S	0	0.009	0.008	1.6E-19

Table 2: Predicted gas composition (mol fraction) at anode effect.

	Laboratory Cell	Industrial Cell Unburnt	Industrial Cell Partially burnt	Industrial Cell Totally burnt
CO_2	0.004	0.004	0.004	0.258
CO	0.632	0.619	0.653	0.318
COS	0.010	0.007	0.007	0.008
S_2	9.1E-04	5.3E-04	4.6E-04	0.002
CS_2	0.006	0.003	0.003	6.0E-05
SO_2	6.8E-10	4.9E-10	5.1E-10	1.8E-05
CF_4	0.311	0.303	0.272	0.171
C_2F_6	9.5E-07	9.1E-07	7.8E-07	2.4E-08
O_2	1.1E-19	1.0E-19	1.1E-19	1.7E-15
H_2	0	0.020	0.019	0.008
H_2O	0	2.0E-04	1.9E-04	0.010
H_2S	0	0.007	0.006	0.006
COF_2	0.037	0.035	0.035	0.217

The assumptions made mean the thermodynamic analysis is indicative only, but the trends it highlights are important. The formation of COS in the unburnt gas and transformation to SO_2 in the totally burnt gas explains why only COS was detected in the laboratory scale cell. With an inert atmosphere there were no oxidising conditions, so SO_2 could not form. The gas scrubbing could be responsible for the lack of CS_2 and S_2 from the laboratory cell, but the reactions of these gases with solid alumina is not known. The small amount of C_2F_6 indicated agrees with the findings of many studies, where the formation is only for a short time and to a lesser extent than CF_4. The large amount of COF_2 indicated at anode effect for totally burnt industrial cell gas is possibly accentuated because of the mass balance constrictions used. However it does show that in the absence of excess carbon or boron nitride (reactions 9, 10, 11), COF_2 is a favoured equilibrium product at cell operating temperatures.

Involvement of Boron nitride.

Because of the presence of BN in the equipment, it has been predicted that BF_3 would be formed if either COF_2 or CF_4 were present (reactions 11 and 12). Thus, out of both general interest and also to test the accuracy of the thermodynamic predictions, the equipment was set to detect BF_3 also. Boron has two main isotopes, 80% at molecular weight 11 and 20% at 10. Thus any boron containing ions will be present in pairs, 1 mass unit apart.

In the lower section of Figure 6 the traces at m/e 68 and 67 correspond to the BF_3^+ ion, and those at m/e 49 and 48 correspond to the BF_2^+ ion. The intensity ratio of 68/67 is the same as 49/48, showing that BF_3 formation did occur immediately the cell went on anode effect. Whilst this indicates it may be due to reaction with CF_4, it does not preclude reaction with COF_2 also. Three experiments at 1.107A/cm^2 showed BF_3 produced only during anode effect, and another two at 0.295A/cm^2 showed BF_3 produced before anode effect along with COF_2. Because of these differing relative gas formations it is uncertain if the reactions forming COF_2 and BF_3 are coupled.

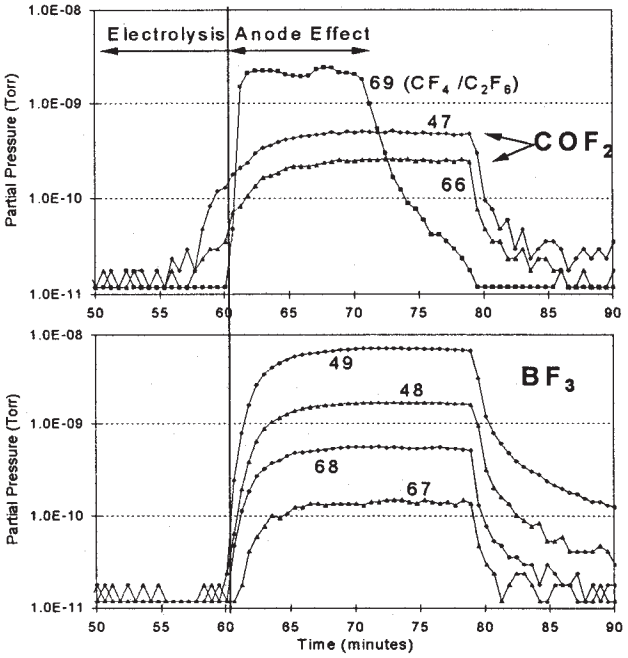

Figure 6: Formation of COF_2 and BF_3.

The fact that BF_3 is formed indicates that the BN in the cell is reacting, although it must be recognised that this is a phenomenon relevant only to laboratory cells containing BN.

Conclusions.

A mass spectrometric system has been used to qualitatively analyse the gases formed in a laboratory scale alumina reduction cell during normal electrolysis and anode effect. In conjunction with this, thermodynamic predictions have been made of the gases formed in both laboratory and industrial cells. The key findings are:

- In the laboratory cell sulfur is released only as COS.
- Thermodynamic analysis indicates that sulfur is initially released as COS, which oxidises to SO_2 as the gas becomes burnt with potroom air.
- CF_4 is only formed during anode effect, none was detected before AE started.
- Thermodynamic analysis indicates a high ratio of CF_4 to C_2F_6 during anode effect.
- COF_2 has been detected immediately prior to anode effect.
- BF_3 has been detected, indicating reactions involving BN, although this is only relevant to laboratory cells.

Acknowledgments.

The authors would like to acknowledge and thank The Comalco Research Services, Melbourne, Australia and The Auckland University Research Committee, Auckland, New Zealand for financial support of this project.

References.

[1] J.L. Henry and R.D. Holliday, "Mass Spectrometric Examination of Anode Gases from Aluminum Reduction Cells," Journal Of Metals, October 1957, 1384-1385.

[2] R. Oedegard, S. Roenning, A. Sterten and J. Thonstad, "Sulphur Containing Species in the Anode Gas from Aluminium Cells," Light Metals 1985, 661-670.

[3] A.T. Tabereaux, "Anode Effects, PFCs, Global Warming, and the Aluminium Industry," JOM, Vol.46, No.11, 1994, 30-34.

[4] A. Øygård, T.A. Halvorsen, J. Thonstad, T. Røe and M. Bugge, "A Parameter Study of the Formation of C-F Gases During Anode Effect in Aluminium Reduction Cells," Light Metals 1995, 279-287.

[5] A.T. Tabereaux, N.E. Richards and C.E. Satchel, "Composition of Reduction Cell Anode Gas During Normal Conditions and Anode Effects," Light Metals 1995, 325-333.

[6] I. Berge, R. Huglen, M. Bugge, J. Lindstrøm and T. Røe, "Measurement and Characterisation of Fluorocarbon Emissions from Alumina Reduction Cells," Light Metals 1994, 389-392.

[7] R.A. Roberts and P.J. Ramsey, "Evaluation of Fluorocarbon Emissions from the Aluminium Smelting Process," Light Metals 1994, 381-388.

[8] F.M. Kimmerle, G. Potvin and J.T. Pisano, "Measured Versus Calculated Reduction of the PFC Emissions from Prebaked Hall Héroult Cells," Light Metals 1997, 165-171.

[9] S.S. Nissen and D.R. Sadoway, "Perfluorocarbon (PFC) Generation in Laboratory-Scale Aluminium Reduction Cells," Light Metals 1997, 159-164.

[10] E.W. Dewing, "The Chemistry of the Alumina Reduction Cell," Canadian Metallurgical Quarterly, Vol.30, No.3, 1991, 153-161.

[11] J. Harnisch, R. Borchers, P. Fabian and K. Kourtidis, "Aluminium Production as a Source of Atmospheric Carbonyl Sulfide (COS)," Environmental Science and Pollution Research, Vol.2, No.3, 1995, 161-162.

[12] J. Harnisch, R. Borchers and P. Fabian, "COS, CS2 and SO2 in Aluminium Smelter Exhaust: The Contribution of Aluminium Production to the Global COS Budget," Environmental Science and Pollution Research, Vol.2, No.4, 1995, 229-232.

[13] F.M. Kimmerle, L. Noël, J.T. Pisano and G. I. Mackay, "COS, CS2 and SO2 Emissions from Prebaked Hall Héroult Cells," Light Metals 1997, 153-158.

[14] M.M.R. Dorreen, M.M. Hyland and B.J. Welch, "An Improved Method for Current Efficiency Determination in a Laboratory Aluminium Cell," Light Metals 1997, 1189-1193.

[15] "ASTM Special Technical Publication 356: Index of Mass Spectral Data Listed by Molecular Weight and the Four Strongest Peaks," American Society for Testing and Materials, Philadelphia, Pa, 1st Edition, July, 1963.

[16] A.J. Calandra, C.E. Castellano and C.M. Ferro, "The Electrochemical Behaviour of Different Graphite/Cryolite Alumina Melt Interfaces Under Potentiodynamic Perturbations," Electrochimica Acta Vol.24, 1979, 425-437.

[17] T.M. Hyde and B.J. Welch, "The Gas Under Anodes in Aluminium Smelting Cells Part I: Measuring and Modelling Bubble Resistance Under Horizontally Oriented Electrodes," Light Metals 1997, 333-340.